# Parametric Study of an Ablative TPS and Hot Structure Heatshield for a Mars Entry Capsule Vehicle

Sarah L. Langston[*], Christopher G. Lang[†], and Jamshid A. Samareh[‡]

*NASA Langley Research Center, Hampton, Virginia, 23681, USA*

The National Aeronautics and Space Administration is planning to send humans to Mars. As part of the Evolvable Mars Campaign, different entry vehicle configurations are being designed and considered for delivering larger payloads than have been previously sent to the surface of Mars. Mass and packing volume are driving factors in the vehicle design, and the thermal protection for planetary entry is an area in which advances in technology can offer potential mass and volume savings. The feasibility and potential benefits of a carbon-carbon hot structure concept for a Mars entry vehicle is explored in this paper. The windward heatshield of a capsule design is assessed for the hot structure concept as well as an ablative thermal protection system (TPS) attached to a honeycomb sandwich structure. Independent thermal and structural analyses are performed to determine the minimum mass design. The analyses are repeated for a range of design parameters, which include the trajectory, vehicle size, and payload. Polynomial response functions are created from the analysis results to study the capsule mass with respect to the design parameters. Results from the polynomial response functions created from the thermal and structural analyses indicate that the mass of the capsule was higher for the hot structure concept as compared to the ablative TPS for the parameter space considered in this study.

---

[*]Research Aerospace Engineer, Structural Mechanics and Concepts Branch, Mail Stop 190, AIAA Member.

[†]Research Aerospace Engineer, Structural Mechanics and Concepts Branch, Mail Stop 190.

[‡]Aerospace Engineer, Vehicle Analysis Branch, Mail Stop 451, AIAA Associate Fellow.

# I.   Introduction

The mission to send humans to Mars may require larger payloads to be delivered to the surface of the planet than previously accomplished. A Mars mission will require novel approaches in entry vehicle design, both in the shaping and architectures of the vehicles and the materials needed.[1] The thermal protection system (TPS) of a planetary entry vehicle is a critical component required to protect the vehicle from the severe aerodynamic heating environment during atmospheric entry. The current state-of-the-art TPS insulates the underlying structure with the use of an ablative material or ceramic tile. The insulating TPS is bonded to an underlying structure that carries the mechanical loads associated with entry. The underlying structure is generally an aluminum or composite sandwich, and room temperature vulcanizing (RTV) adhesive is used to bond the TPS to the sandwich structure. Ablators are considered semi-passive TPS materials. They are single use, but are able to withstand higher heating rates than reusable TPS such as the ceramic tiles used on the space shuttle orbiter.[2,3] The use of ablators manages the thermal loads in multiple ways. Heat is both blocked by ablation and absorbed during the ablation process.[2,3] An ablative TPS was used by the Apollo missions and is in current use on the Orion capsule. Previous spacecraft sent to the surface of Mars have utilized an ablative TPS such as the Mars Science Laboratory (MSL) mission.[4–6]

Hot structures are high temperature materials which provide load carrying capability at elevated temperatures. For entry vehicles, hot structures do not require additional thermal protection on the outer surface of the vehicle. Potential applications for hot structures include nose caps, control surfaces, heatshields, and aeroshells for planetary entry. Lightweight high temperature insulation can be used underneath hot structures to protect the interior when required.[2,3] Unlike ablative TPS where the outer surface ablates, hot structures have little to no change in their outer mold line geometry during use, thus, there is potential for reusability. The hot structure concept in this study consists of an advanced carbon-carbon (ACC) material on the outer surface of the vehicle with lightweight flexible insulation and a Nextel fabric liner included underneath the hot structure.[7,8] In this hot structure concept, ACC provides some thermal protection while carrying the primary strutural loads experienced during entry. The required amount of lightweight blanket insulation is included to maintain an internal temperature limit. Due to the multifunctionality of the hot structure concept with the use of lightweight internal insulation, there is potential for both mass and volume savings.

Previous studies[7,8] have been completed both comparing state-of-the-art point designs for an ablative TPS and the hot structure concept, using parametric models to investigate different vehicle designs.[7–12] A comparison study was performed on the MSL heatshield,[8]

the Hypersonic Inflatable Aerodynamic Decelerater (HIAD) rigid nose cap, and a Mid Lift-to-Drag (Mid L/D) vehicle.[9] The hot structure concept, as compared to an ablative TPS, showed a lower mass for the MSL heatshield and Mid L/D aeroshell applications and an increased mass for the HIAD nose cap. All three vehicles had volume savings with the hot structure concept. Another study was performed on the Mid L/D design using a parametric model to determine the impact to the ablative TPS due to vehicle geometry and structural stiffener arrangement.[10,11] Parametric studies focusing on mass modeling for Mars EDL were also performed.[12]

Vehicles being considered for reaching the surface of Mars include evolutions of state-of-the-art capsule designs flown to Mars, novel vehicles that expand the heatshield area, and lifting body vehicles. In this paper, the hot structure concept was compared to an ablative TPS using parametric models for the heatshield capsule entry vehicle with a diamter of 9.85 meters.[13] The influence of vehicle design parameters on the overall vehicle mass was studied by varying parameters associated with the vehicle geometry, payload, and thermal loading conditions. The minimum mass design was determined by performing thermal and structural finite element analyses. Multiple designs were analyzed within the parameter space, and the output of capsule mass from the analysis model was collected for various values of the design parameters. This collection of data was used to create a second order polynomial response functions[14] using least squares regression methods[14] as a function of the design parameters. The output of the polynomial response function is the capsule mass. The response functions were used to study the influence of the design parameters on the vehicle mass.

## II.  Capsule Vehicle Design

Capsule designs have historically been used in Mars missions, including the MSL mission.[4,5] The Jet Propulsion Laboratory (JPL) has designed a capsule that is larger than previous missions, but maintains the heritage of the capsule design.[13] The outer mold line shape of the capsule design consists of a heatshield on the windward surface of the vehicle and a backshell. The geometry of the heatshield and backshell are depicted in Figure 1, with lines showing the structural stiffener arrangement of rings and longerons. The baseline geometry of the heatshield was a diameter of 9.85 meters and a height of 8 meters measured from the backshell apex to the center of the heatshield. Interior to the capsule is a frustum to provide structural support and payload attachment.
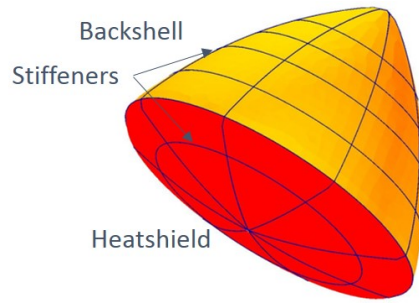
Figure 1: The outer mold line for the capsule design depicting the heatshield and backshell regions with internal ring and longeron structural stiffeners.

## III.    Thermal Protection Systems

### A.    Heatshield Concepts

The heatshield concepts chosen for evaluation in this study are depicted in Figure 2. The ablative TPS concept consists of an ablator material bonded to a honeycomb sandwich composite carrier structure. Phenolic impregnated carbon ablator (PICA)[15] is used for the ablator material. The PICA is bonded to a carrier structure using RTV-560 adhesive. The carrier structure consists of IM7 graphite facesheets and a 5052 alloy hexagonal aluminum honeycomb core. This stack-up is consistent with the heatshield layup flown on the MSL in terms of the components including the PICA ablator, honeycomb composite carrier structure, and RTV bonding agent.[4,5,8] The material chosen for the hot structure concept was advanced carbon carbon that has undergone six pyrolysis cycles (ACC-6). Underneath the ACC-6 is a layer of opacified fibrous insulation (OFI),[16] which is held in place by a layer of Nextel fabric. Jettison of the heatshield after aerocapture or during entry is not considered in this study.



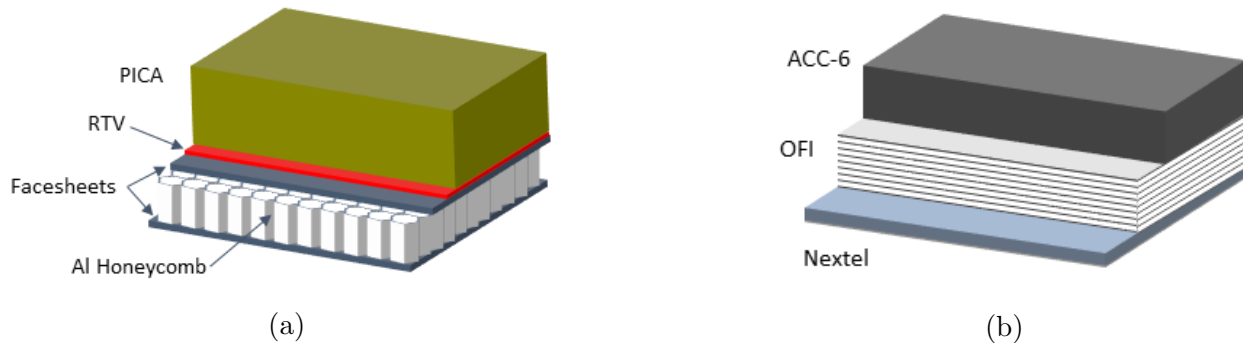(a)                                                                                   (b)

Figure 2: Schematic of the (a) ablative TPS and (b) hot structure concept.

## B.  Backshell Concept

The backshell TPS selected for this study is depicted in Figure 3.  The backshell TPS consisted of SLA-561,[17] which is a low density ablator material. While SLA-561 is an ablative material, it is not predicted to ablate for this study.  The scaled heat fluxes applied to the backshell of the capsule result in a low peak surface temperature as compared to the heatshield. The SLA-561 is bonded to an Al-2024 skin using RTV-560.[5]
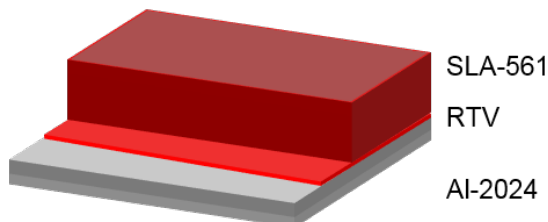


Figure 3: Schematic of the backshell TPS.

# IV.   Models and Methodology

## A.  Thermal Models

The heatshield thermal analysis was performed using the Fully Implicit Ablation and Thermal Response program (FIAT).[18] FIAT is a one-dimensional transient ablation and thermal analysis and sizing code for multilayer TPS and multifunctional hot structure concepts subject to aeroheating on the outer surface of the heatshield. The thermal analysis accounts for pyrolization, ablation, recession of the outer surface material, and heat conduction through the layers.  The stagnation pressure was used for the ablation and gas conduction model through the PICA material, because PICA is exposed to the stagnation pressure on the outside of the vehicle. For the hot structure concept, the OFI material was analyzed using the atmospheric pressure for the gas conduction model through the OFI material which was subject to the wake pressure as it was underneath the ACC-6 material. The wake pressure was lower or equal to the atmospheric pressure.

The heat flux data input to the thermal analysis was applied to the outer surface of both the ablative TPS and hot structure concept for each trajectory.  An adiabatic boundary condition was assumed at the inner surface. The outer surface aero heating convective and radiative heat fluxes were specific to the vehicle trajectory, which included an aerocapture and entry phase.  The convective and radiative heat fluxes are based on two-dimensional axisymmetric LAURA and HARA computational aerothermodynamic solutions[19] and were computed at the stagnation point.  The heating profile shown in Figure 4 combines both the radiative and convective components and was separated into the aerocapture and entry

trajectories. For this study, the heat loads had a factor of safety of 1.5 and 1.4 for the radiative and convective components, respectively.[20] A cooling period was added for each trajectory since the peak internal temperature may occur after the heating period. The cooling period consisted of radiation and convection at the material surface for entry and only radiation for aerocapture. For the thermal analysis, the heating data for multiple trajectories were analyzed. The capsule trajectories varied the ballistic coefficient for the aerocapture and entry phases of planetary entry. The baseline ballistic coefficient for the aerocapture and entry trajectories was 560 kg/m$^2$. The ballistic coefficient was varied between 100 kg/m$^2$ and 700 kg/m$^2$ for aerocapture. The entry ballistic coefficient was varied by 80% of the baseline, 100% of the baseline, and 120% of the baseline. The heat fluxes for the baseline ballistic coefficients during aerocapture and entry are shown in Figure 4. The peak heat flux varied 26-119% and 87-117% due to the variation in ballistic coefficient for aerocapture and entry, respectively.
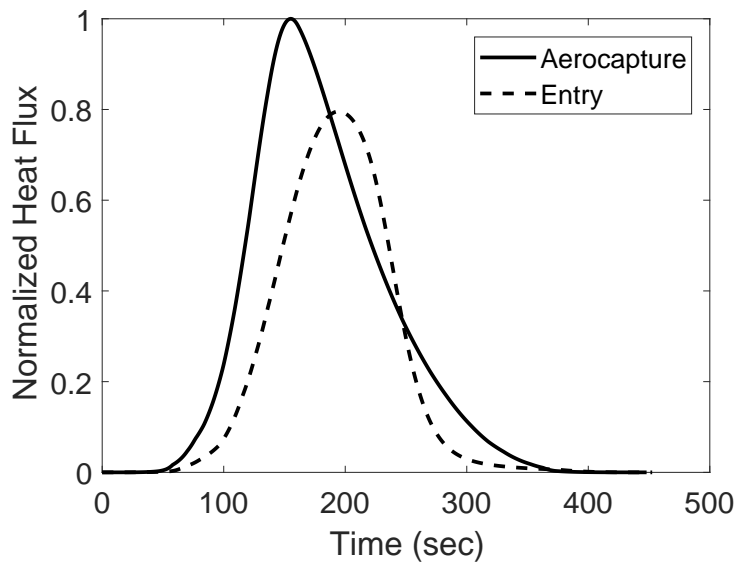


Figure 4: Heat flux for the baseline aerocapture and entry trajectory, normalized with respect to the maximum heat flux for entry.

The heatshield thermal analysis sized the thickness of the PICA for the ablative TPS and the thickness of OFI for the multifunctional hot structure concept. Both designs were sized subject to the material temperature constraints listed in Table 1. For the ablative TPS, the RTV layer was held at a constant thickness of 0.3 millimeters. The composite facesheets and aluminum core of the substructure were held constant at their minimum material thickness values of 1 millimeter and 20 millimeters, respectively. For the multifunctional hot structure

concept, the Nextel layer was held constant at 0.5 millimeters. The ACC-6 thickness was held constant during the analysis at 6.35 millimeters.

The backshell thermal analysis was performed using a one-dimensional transient finite element method conduction code, and the thickness of the SLA-561 was sized according to the bondline temperature constraint listed in Table 1. The heat fluxes applied to the heatshield were scaled by 5% for the backshell to represent the reduced heating on the backshell of the capsule. The RTV was held at a constant at 0.3 millimeters and the Al-2024 was held at 6.35 millimeters.

Table 1: The thermal sizing temperature constraints for the ablative TPS and hot structure concept heatshields.

| | |
|---:|:---|
| Ablative TPS Heatshield | 260°C at RTV-560 |
| Hot Structure Concept Heatshield | 150°C at Nextel Fabric |
| Backshell | 260°C at RTV-560 |

## B.  Structural Finite Element Model (FEM)

A linear static and buckling analysis was performed using Nastran[21] finite element software to determine the stress distribution and buckling eigenvalues given the aerodynamic and inertial loads for launch and entry load cases. The capsule design finite element model (FEM) included the heatshield, backshell, and frustum sections. Each of the sections in the capsule vehicle model were stiffened, and the finite element model is depicted in Figure 5. The heatshield is stiffened by two rings and eight longerons. The inner heatshield ring is located at the interface with the frustum, and the outer heatshield ring is located at the interface with the backshell. The backshell is stiffened by four rings and eight longerons, and the frustum includes an upper ring and eight longerons. Both the ablative TPS and hot structure concept heatshields were evaluated.

For the finite element models, shell elements were used to model the ablative TPS carrier structure and the hot structure concept skin. The shell element properties for the ablative TPS represented a symmetric sandwich composite with graphite facesheets and an aluminum honeycomb core. The PICA and RTV were uniformly distributed as non-structural mass for the shell elements. The shell element properties for the hot structure concept were approximated by in-plane isotropic properties for ACC-6, and the OFI and Nextel fabric were included as non-structural mass uniformly distributed over the shell elements. The heatshield ablative TPS and hot structure concepts included structural stiffeners with blade cross-sections. The stiffeners were modeled using beam elements with Al-2024 and ACC-6 properties for the ablative TPS and hot structure concept, respectively. Shell elements were

also used to model the backshell and frustum with Al-2024 properties. SLA-561 and RTV were included on the backshell as uniformly distributed non-structural mass for the shell elements. The stiffeners were modeled as beam elements with blade cross-sections and Al-2024 properties. The payload mass was distributed equally as point masses on the frustrum upper ring.

Two structural loading cases were applied to the capsule FEM, Earth launch and Mars entry. For this study, the vehicle would not be launched within a shroud and therefore a pressure load was included for each load case. Earth launch and Mars entry pressure loads where computed using the modified Newtonian sine-squared law.[10] This method to compute the pressure distribution is considered a reasonable approximation for determining hypersonic aerodynamic loads. The modified Newtonian sine-squared law takes into account the curvature of the capsule and the vehicle angle of attack to the flow to determine the appropriate pressure load for each element. The model assumed a zero degree angle of attack for both launch and entry. Launch acceleration loads were applied as 5 times the acceleration of gravity in the axial direction and 0.25 times the acceleration of gravity in the lateral direction. For the launch load case, a clamped boundary condition is applied to the inner heatshield ring corresponding to the attachment interface for the launch vehicle. Inertial relief is applied for the Mars entry load case to generate the forces necessary for static equilibrium of the vehicle.

The capsule geometry, payload mass, heatshield insulation thickness, and backshell insulation thickness were varied in the parametric analysis. The capsule geometry was scaled uniformly in all directions. The baseline values of the four parameters are listed in Table 2, as well as the parameter space studied.

Table 2: The baseline parameter values, and design space for the parametric model.

| Parameter | Baseline Value | Parameter Space |
|:---:|:---:|:---:|
| Geometry Scale | 9.85 m diameter / 8 m height | 0.7-1.0 scale factor |
| Payload Mass | 54.09 metric tons | 15-60 metric tons |
| Heatshield Insulation Thickness | 1.86 cm [PICA] / 3.5 cm [OFI] | 1.5-3.5 cm PICA / 2.54-7.62 cm OFI |
| Backshell Insulation Thickness | 0.635 cm [SLA-561] | 0.635-2.6 cm SLA-560 |

The geometry parameter space was chosen in accordance with expected launch vehicle designs. Current launch vehicle designs estimate a 9.85 m vehicle diameter limit. This study considered smaller entry vehicles that could be launched on potentially smaller launch

vehicles. The payload mass parameter space was chosen to identify the effect of delivering larger and smaller payloads. The payload parameter includes the payload being delivered as well as additional internals such as fuel, electronics, and structural systems. The insulation parameter space for both the heatshield and the backshell were derived from the result of the thermal analysis discussed in Section A.
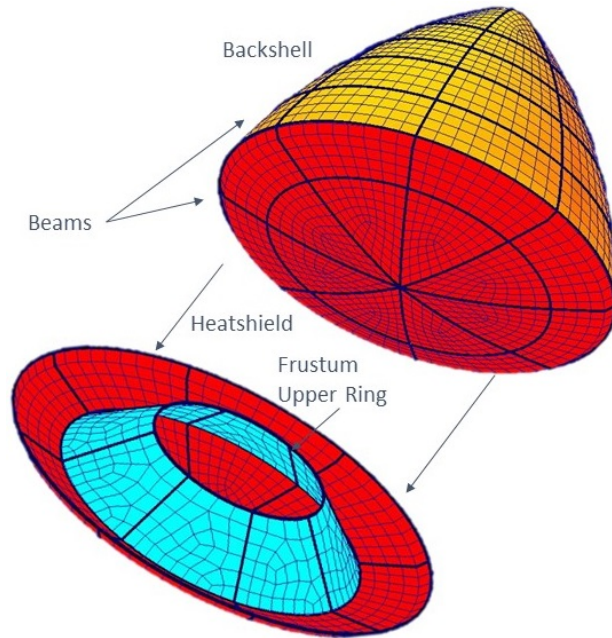


Figure 5: Finite element mesh of the capsule vehicle.

## C.   Structural Optimization Process

Nastran solution 200[22] was utilized to optimize the skin thickness for the heatshield, frustum, and backshell sections and the ring and longeron stiffener dimensions for the minimum structural mass given constraints on the material stress limit and critical buckling load. The structural optimization analysis design variable initial values used in this study are listed in Table 3, along with their minimum and maximum bounds. The minimum and maximum material bounds were chosen as reasonable approximations of manufacturability. The thermal sizing analysis provided the bounds for the TPS thickness which was used as a structural analysis design space parameter.

Table 3: The structural optimization design parameter's initial value, and minimum and maximum bounds for the capsule FEM.

| Design Variable | Initial Value (m) | Minimum Bound (m) | Maximum Bound (m) |
|---|---|---|---|
| *Stiffeners* | | | |
| Longeron Height | 0.0127 | 0.0127 | 0.05 |
| Longeron Width | 0.0127 | 0.0127 | 0.05 |
| Heatshield Ring Height | 0.0127 | 0.0127 | 0.05 |
| Heatshield Ring Width | 0.0127 | 0.0127 | 0.05 |
| Frustum Stiffeners Height | 0.0127 | 0.0127 | 0.05 |
| Frustum Stiffeners Width | 0.0127 | 0.0127 | 0.05 |
| Backshell Ring Height | 0.0127 | 0.0127 | 0.05 |
| Backshell Ring Width | 0.0127 | 0.0127 | 0.05 |
| *Skin Thicknesses* | | | |
| Backshell Skin Thickness | 0.00635 | 0.00635 | 0.05 |
| ***Ablative TPS*** | | | |
| Heatshield Facesheet Thickness | 0.001 | 0.001 | 0.02 |
| Heatshield Core Thickness | 0.02 | 0.02 | 0.2 |
| Frustum Skin Thickness | 0.00635 | 0.00635 | 0.05 |
| ***Hot Structure Concept*** | | | |
| Heatshield Thickness | 0.0254 | 0.002159 | 0.0254 |
| Frustum Skin Thickness | 0.05 | 0.00635 | 0.05 |

The solution 200 optimization is sensitive to the initial values given to the design parameters. Initially, the frustum and heatshield skin thicknesses in the hot structure concept were set at the minimum bound for the initial value, however it was found that the optimizer was consistently unable to find a feasible design with those initial conditions. Therefore, the frustum and heatshield skin thicknesses were initialized at the maximum bound during the hot structure concept optimization to help facilitate the optimizer finding a feasible design. The initial specific design variable values for this study are listed in Table 3.

The objective function for this optimization was to minimize the structural mass of the vehicle. The optimized structural mass was the total mass of the vehicle minus the payload, which was modeled as distributed point masses within the FEM. This objective function was subject to multiple constraints. The constraints included limits for the von

Mises stress with a 1.4 factor of safety applied. For the ablative TPS this included material stress limits for the IM7 facesheets, Aluminum honeycomb core, and Al-2024. For the hot structure concept this included material stress limits for the ACC-6, and Al-2024. Both the ablative TPS and hot structure concept were also subject to a buckling load constraint. A multiplying factor was placed on the critical buckling load. This multiplying factor was based on empirical formulas for the buckling of a stiffened shell based on geometry and material property values.[23] The ablative TPS applied a multiplying factor of 1.79 to the critical buckling load and the hot structure design applied a multiplying factor of 3.7. It is important to note that there was no constraint placed on the displacement or bending of the heatshield. This is particularly noteworthy for the ablative TPS design, where a large displacement of the underlying carrier structure may cause a critical failure of the TPS bond or fracture of the PICA material. Inclusion of a displacement constraint could change the results and conclusions for this study.

## D.   Polynomial Response Functions

Polynomial response functions[14] were created for the structural sizing response of the capsule design. The response functions were a polynomial regression where the coefficients were determined by the least-squares approach.[14] The polynomial response function provided an expected output value in terms of a vector of independent design variables. A separate response function was created for the optimized vehicle mass with the ablative TPS and the hot structure concept heatshield by varying the payload, capsule size, and TPS thickness. Polynomial response functions were created due to the large parameter space being studied and the analysis time required for each design sample point analyzed. Depending on the machine being used to compute the analysis and the specific structural inputs, the optimization of the finite element model could take up to 15 minutes to complete. These parameters made it time prohibitive to fully characterize the parameter space by analyzing every possible combination of parameters. The creation of response functions allowed for a continuous study of the design space, rather than a discrete approach.

The thermal sizing analysis and structural optimization models in the preceding sections were used to build the polynomial response functions. A visual depiction of the methodology used to crate the polynomial response functions is shown in Figure 6. The design space parameters consisted of the TPS thickness, vehicle geometry scale, and payload mass. Latin Hypercube Sampling[24] (LHS) of these design space parameters was performed and the structural optimization analysis provided the minimum mass for each sample. The parameters were independent with a uniform probability distribution for sampling. The structural analysis was subject to optimization for a minimum vehicle structural mass objective function. The design space parameters and corresponding optimized vehicle mass were collected and
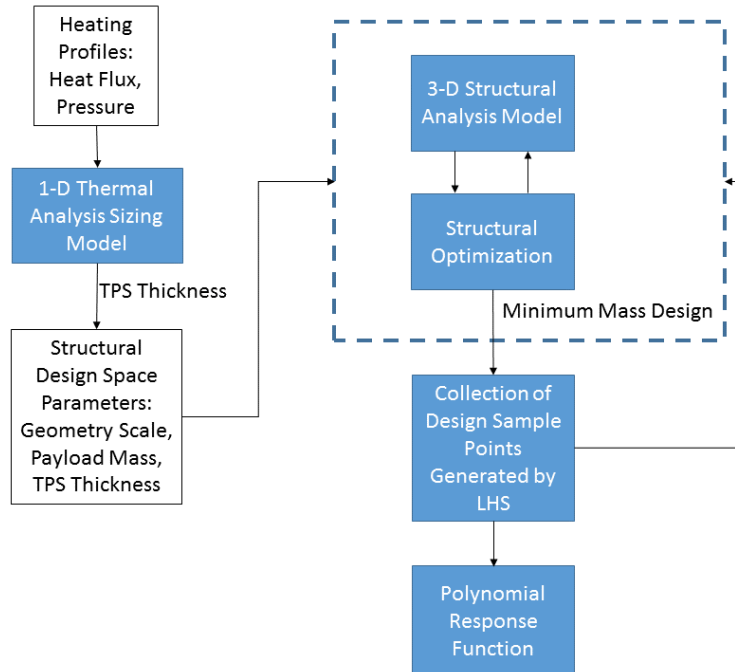
used to create a polynomial response function.



Figure 6: Flow chart of the analysis methodology used for the parametric study of the capsule design.

The response functions were constructed for the optimized mass of the capsule. The total vehicle mass was used, rather than just the heatshield mass, to capture the effects of the heatshield on the rest of the vehicle design. A design sample point in this study is defined as the as optimized vehicle mass derived from LHS chosen parametric inputs. The ablative TPS heatshield used LHS to generate 500 design sample points to create the polynomial response function. The hot structure concept used LHS to generate 400 design sample points to create the polynomial response function. The difference in the number of design points generated for each design was due to analysis computation time. For both the ablative TPS and hot structure concept, a quadratic response function was determined as sufficient for this study. Using higher order functions did not significantly reduce the maximum or average errors. The quadratic response along with the ideal response are shown in Figure 7. The PICA structural response function has a maximum error of 2.76%, while the hot structure response function has a higher maximum error of 5.23%. The average error for both the ablative TPS and hot structure concept capsule response functions is below 1.5%.
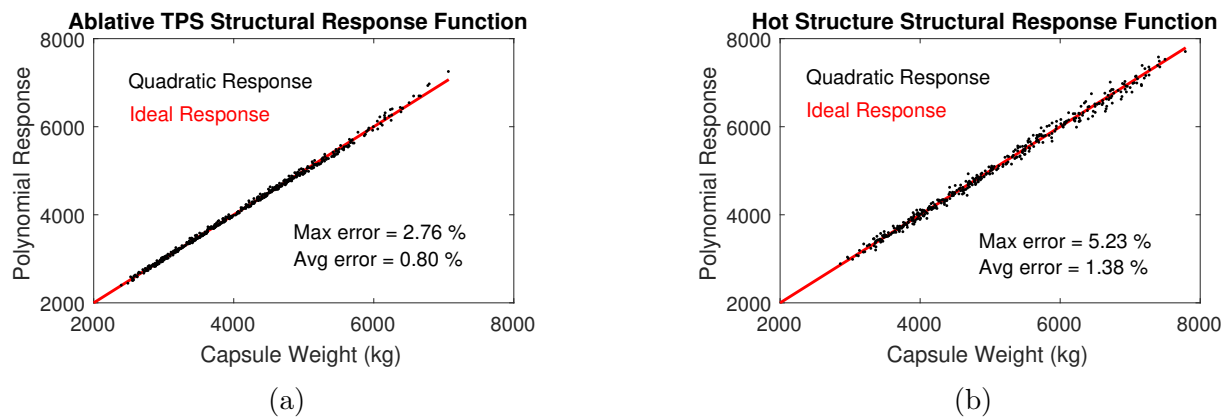
Figure 7: Structural response function output of the (a) ablative TPS and (b) hot structure concept for the capsule design compared to the ideal response.

# V.   Results

## A.   Thermal Analysis Results

The one-dimensional thermal analysis outlined in Subsection A in the Models and Methodology section sized the thickness of the PICA and OFI for the capsule heatshield and the SLA-561 for the backshell. The insulations were sized subject to the temperature constraints given in Table 1. The thicknesses of the other materials in each TPS design remained constant. The surface temperatures and the TPS thicknesses required for the basline load case as well as the TPS thickness bounds required for a range of ballistic coefficients is presented.

The surface and RTV bondline temperatures of the ablative TPS for aerocapture and entry are shown in Figure 8 for the baseline trajectory using the minimum PICA thickness required for the bondline temperature constraint. While the cooling period extended to 6000 seconds, only the first 1000 seconds are shown which includes the peak bondline temperature. The required PICA thickness for aerocapture was predicted as 2.90 cm while the required PICA thickness for entry was 2.28 cm. The maximum surface temperature reached during aerocapture was higher, which corresponded to a larger PICA thickness for aerocapture than for entry. The bondline temperature reached a maximum near the end of the heating period and declined during the cooling period. The predicted recession amount at the surface was 0.627 cm and 1.03 cm for aerocapture and entry, respectively.
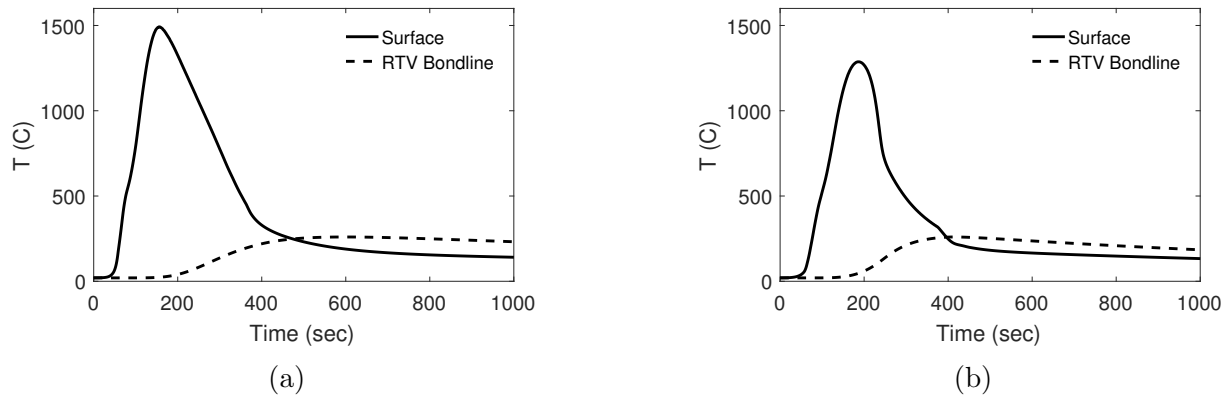
Figure 8: The surface and bondline temperatures for the ablative TPS during the first 1000 seconds of the (a) aerocapture and (b) entry baseline trajectories.

The surface temperature and backface temperature for the hot structure concept are shown in Figure 9 for aerocapture and entry. The minimum thickness of OFI was predicted to be 3.95 cm for aerocapture and 5.05 cm for entry. The cooling period extended to 6000 seconds after the end of the heating period, and the peak temperature at the backface is reached during the cooling period. For the hot structure concept, the backface temperature reaches a maximum during the cooling period and slowly declines due to the insulated boundary condition and the OFI. The backface temperature declines slower for aerocapture due to the absence of convection for cooling at the surface. While the peak backface temperature for aerocapture is near the end of the cooling period, additional cooling shows the backface temperature remains approximately constant. Additionally, the insulated boundary condition at the backface leads to a conservative estimate of the required OFI thickness. Little to no recession occurs at the surface of the ACC-6 and is estimated as less than 0.2 cm. The required thickness of the SLA-561 for the backshell was estimated as 0.672 cm and 0.847 cm for the aerocapture and entry baseline trajectories, respectively.
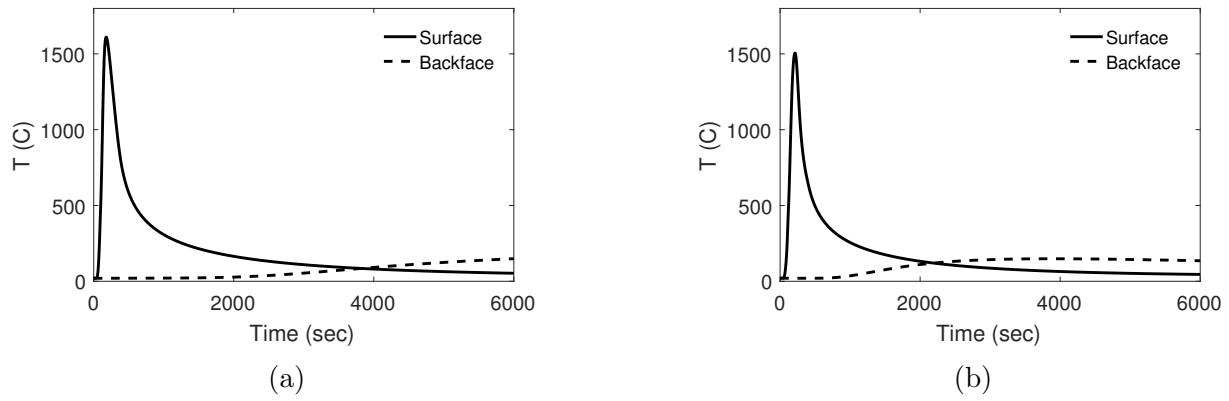
Figure 9: The surface and backface temperatures for the hot structure concept during the (a) aerocapture and (b) entry baseline trajectories.

In order to estimate a range of insulation thicknesses, multiple heat flux and pressure profiles were determined by varying the ballistic coefficient. The ballistic coefficient was varied from 100 kg/m$^2$ to 700 kg/m$^2$ for aerocapture and 80% to 120% of the baseline for entry which corresponds to 448 kg/m$^2$ to 627 kg/m$^2$. The minimum thickness of the PICA, OFI, and SLA-561 were determined for each trajectory, and the thicknesses as a function of the ballistic coefficient are shown in Figure 10. Because the maximum heat flux and total heat load increase with ballistic coefficient, the peak surface temperature and required insulation is predicted to increase as the ballistic coefficient increases. It was from this data that the bounds for the parameter space for the insulation thicknesses were derived.
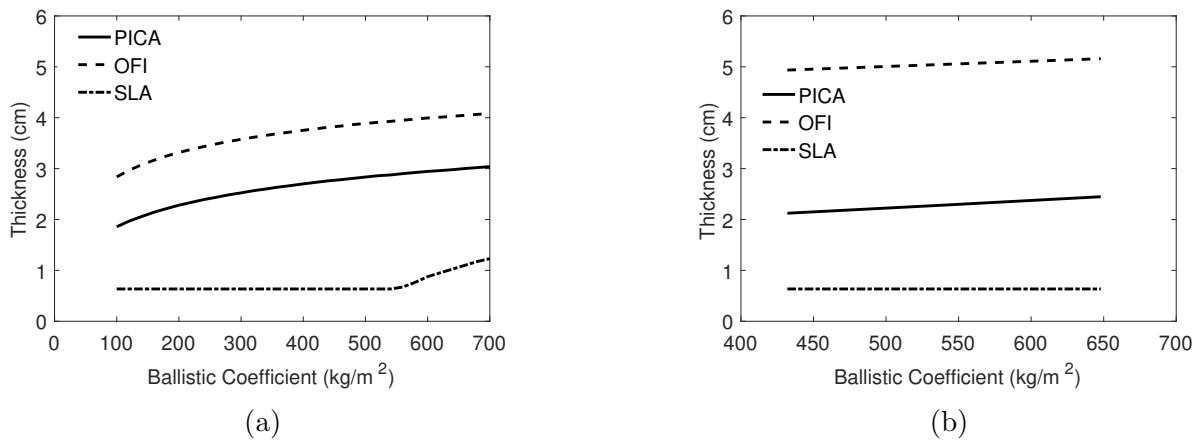


Figure 10: The required PICA, OFI, and SLA-561 thicknesses for (a) aerocapture and (b) entry with varying ballistic coefficient.

## B.  Structural Optimization Results

At the baseline parameter values shown in Table 2, the capsule with an ablative TPS heatshield was 27% lower mass than the capsule with a hot structure concept heatshield. The optimized design variable values for the ablative TPS heatshield capsule and hot structure concept heatshield capsule are shown in Table 4 using the baseline parameter values. The associated total mass and section mass are shown in Table 5.

Table 4: The optimized structural design variables for the ablative TPS and hot structure concept capsule.

| Design Variable | Ablative TPS (m) | Hot Structure Concept (m) |
|---|---|---|
| *Stiffeners* | | |
| Longeron Height | 0.0127 | 0.0127 |
| Longeron Width | 0.0127 | 0.0127 |
| Heatshield Ring Height | 0.0315 | 0.0127 |
| Heatshield Ring Width | 0.0261 | 0.0127 |
| Frustum Stiffeners Height | 0.05 | 0.05 |
| Frustum Stiffeners Width | 0.05 | 0.05 |
| Backshell Ring Height | 0.0127 | 0.0127 |
| Backshell Ring Width | 0.0127 | 0.0127 |
| *Skin Thicknesses* | | |
| Frustum Skin Thickness | 0.020 | 0.0321 |
| Backshell Skin Thickness | 0.00635 | 0.00635 |
| ***Ablative TPS*** | | |
| Heatshield Facesheet Thickness | 0.004 | – |
| Heatshield Core Thickness | 0.037 | – |
| ***Hot Structure Concept*** | | |
| Heatshield Thickness | – | 0.0141 |

From Table 4 the differences in the design variables can be compared for the ablative TPS and hot structure concepts. The stiffeners, with the exception of the heatshield ring frames, were all the the same dimensions between designs. The backshell thickness was also constant at the minimum variable bound for each design. There were, however, differences in the frustum skin thickness between the ablative TPS and hot structure concept.

Table 5: The total and section mass of the optimized structure for the ablative TPS and hot structure concept capsule at the baseline parameter values.

| Section | Ablative TPS (kg) | Hot Structure Concept (kg) |
|---|---|---|
| Backshell | 3053 | 3053 |
| Frustum | 2199 | 3403 |
| Heatshield | 1724 | 2407 |
| Total | | |
| | 6977 | 8863 |

In Table 5 the differences between the total mass and the individual section mass for each design can be compared. The backshell remained the same for each design, while the heatshield and frustum was heavier for the hot structure concept, leading to an overall heavier vehicle mass. In the ablative TPS, the heatshield accounts for 25% of the mass, and in the hot structure concept the heatshield accounts for 27% of the mass. The optimized mass ignores any displacement constraint for the bending of the ablative TPS heatshield which may impact the optimized mass. The potential volume savings can also be investigated by comparing the thicknesses of the heatshields. The ablative TPS heatshield is 6.36 cm thick and the hot structure concept heatshield is 4.92 cm thick. The thickness of the ablative TPS accounts for the two facesheets, core, RTV, and PICA thicknesses. The hot structure thickness is calculated from the ACC-6, OFI, and Nextel thicknesses. If the outer mold line of the vehicle is assumed to remain constant between the two heatshield designs, the thinner hot structure concept would have a larger internal volume than the ablative TPS heatshield.

## C.   Parametric Study Results

The response functions described in Subsection D of the Models and Methodology section were studied to understand the impact of varying different design parameters. The response functions for the capsule design were used to study the effect of the geometry size, payload mass, and insulation thickness on the structural mass of the vehicle. The structural mass of the vehicle included the heatshield, backshell, and frustum without the payload. The baseline geometry corresponds to a scale factor of one. The capsule response models were studied by focusing on one individual parameter at a time while holding the other two parameters constant at their maximum, minimum, or mean value. The baseline values and parameter space for the four parameters in this study are listed in Table 2.

The figures throughout this section show the ablative TPS in blue and the hot structure concept in red. The response models exhibited similar behavior for the maximum, minimum, and mean spectrum. Therefore, only the mean value results will be shown in subsequent figures.

The effect of varying the geometry on the capsule mass is shown in Figure 11. The hot structure concept has an increased mass as compared to the ablative TPS for all geometry sizes considered. The difference in mass between the hot structure concept and ablative TPS decreases as the size of the capsule is reduced. At the baseline geometry of the capsule, with the payload mass and TPS thicknesses at their mean values, the ablative TPS has a 25% lower mass than the hot structure concept.

The effect of payload mass on the capsule mass is depicted in Figure 12. The hot structure concept is heavier than the ablative TPS for all payload mass values considered. The capsule mass for the ablative TPS is increasing at a higher rate with respect to the payload mass as compared to the hot structure concept. The response model shows an increase in the capsule mass below a payload mass of 20 metric tons. Additional analyses show that the behavior of the ablative TPS with respect to payload mass reaches a minimum near the lower end of the payload parameter space and does not increase below 20 metric tons. Two contour plots of the effect of the payload mass and geometry scale parameters on the capsule mass for both the ablative TPS and hot structure concept are shown in Figure 13. The geometry size has a more significant impact on the capsule mass than the payload mass for the ablative TPS and hot structure concept in the parameter space studied.

The effect of the heatshield insulation thickness on the capsule mass was minimal. For the ablative TPS, the variation in PICA thickness resulted in less than a 7% difference in total capsule mass in the study. For the hot structure concept, the variation in OFI thickness resulted in less than a 2% difference in capsule mass. For the entirety of the heatshield insulation thickness design space studied, the ablative TPS was also found to be lighter than the hot structure concept. The effect of varying the backshell insulation thickness was found to have a negligible effect on the vehicle design.
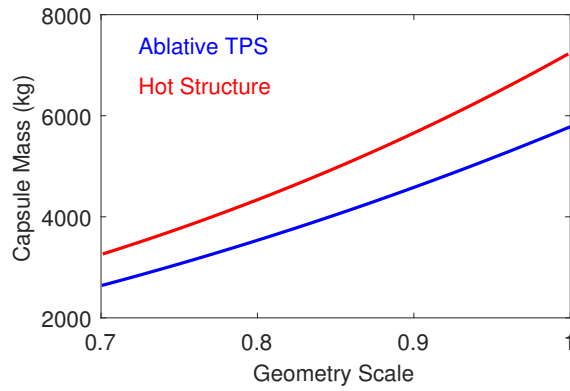
Figure 11: The effect of varying the geometry on the capsule design. The baseline geometry is at the scale factor of one.
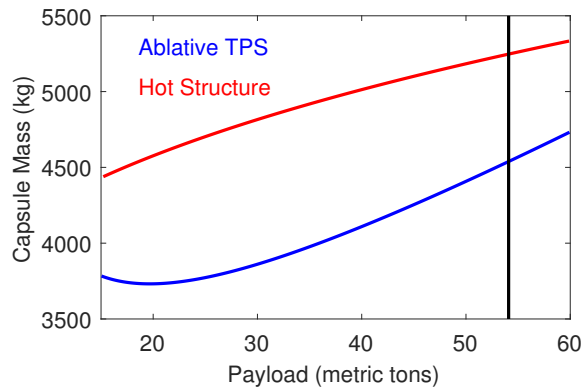


Figure 12: The effect of varying the payload mass carried by the capsule design. The vertical black line is at the baseline payload value of 54.09 metric tons.
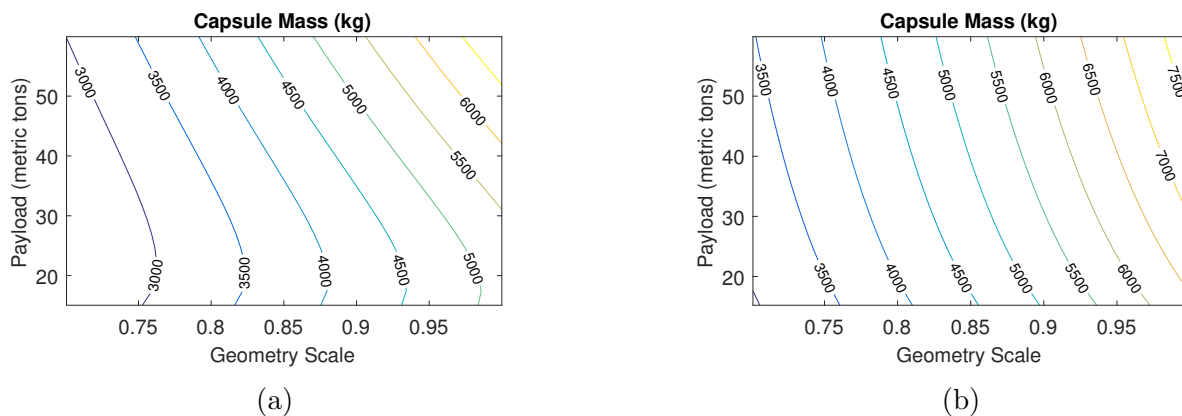


(a)



(b)

Figure 13: Contour plots for the effect of the geometry and payload mass on the capsule mass for the (a) ablative TPS heatshield and (b) hot structure concept heatshield for the capsule vehicle.

# VI.   Concluding Remarks

A parametric study of an ablative TPS and a hot structure concept for the heatshield of a capsule design was presented. The design parameters considered for the capsule included geometry, payload mass, and insulation thickness. The ablative TPS has a lower mass as compared with the hot structure concept for the baseline values of the design parameters for the capsule. At the same baseline designs, the ablative TPS was thicker, therefore the baseline hot structure concept may have volume savings. The ablative TPS also resulted in a lower mass design for all design cases considered. The capsule design showed a similar response for the vehicle mass for the minimum, maximum, and mean of the design space.

There are many opportunities for future work within this research. Higher fidelity analysis models need to be created, and additional structural constraints, such as heatshield deflection, should be considered. The design spaces can be updated, and the coupling of design parameters can be investigated. The analysis could be refined by coupling the thermal and structural analysis in order to take into account thermal stresses. This work can also be expanded to additional vehicles and other configurations, such as a HIAD nose cap or a Mid Lift-to-Drag vehicle.

# Acknowledgments

# References

[1]Dwyer, A. M. et al., "Entry, Descent and Landing Systems Analysis Study: Phase 1 Report," NASA TM-2010-216720, 2010.

[2]Glass, D. E., "Ceramic Matrix Composite (CMC) Thermal Protection Systems (TPS) and Hot Structures for Hypersonic Vehicles," AIAA Paper 2008-2682, April 2008.

[3]Blosser, M. L., *Advanced Metallic Thermal Protection Systems for Reusable Launch Vehicles*, Ph.D. Dissertation, University of Virginia, Charlottesville, VA, May 2000.

[4]Wright, M. J. et al., "Sizing and Margins Assessment of the Mars Science Laboratory Aeroshell Thermal Protection System,"  AIAA Paper 2009-4231, June 2009.

[5]Edquist, K. T., Dyakonov, A. A., Wright, M. J., and Tang, C. Y., "Aerothermodynamic Design of the Mars Science Laboratory Heatshield,"  AIAA Paper 2009-4075, June 2009.

[6]Willcockson, W. H., "Mars Pathfinder Heatshield Design and Flight Experience," *Journal of Spacecraft*

*and Rockets*, Vol. 36, No. 3, May-June 1999, pp. 374–379.

[7]Walker, S. P., Daryabeigi, K., Samaerh, J. A., Armand, S. C., and Periono, S. V., "Preliminary Development of a Multifunctional Hot Structure Heat Shield," AIAA Paper 2014-0350, January 2014.

[8]Walker, S. P., Daryabeigi, K., Samareh, J. A., Wagner, R., and Waters, W. A., "A Multifunctional Hot Structure Heatshield Concept for Planetary Entry," AIAA Paper 2015-3530, July 2015.

[9]Langston, S. L., Lang, C. G., Samareh, J. A., and Daryabeigi, K., "Optimization of a Hot Structure Aeroshell and Nose Cap for Mars Atmospheric Entry," AIAA Paper 2016-5594, September 2016.

[10]Lane, B. M. and Ahmed, S. W., "Parametric Structural Model for a Mars Entry Concept," NASA TM-2017-219375, 2017.

[11]Ahmed, S. W. and Lane, B. M., "Finite Element Modeling and Analysis of Mars Entry Aeroshell Baseline Concept," NASA TM-2017-219374, 2017.

[12]Samareh, J. A. and Komar, D. R., "Parametric Mass Modeling for Mars Entry, Descent and Landing System Analysis Study," AIAA Paper 2011-1038, January 2011.

[13]Price, H. W., Braun, R. D., Manning, R., and Sklyanski, E., "A High-Heritage Blunt-Body Entry, Descent, and Landing Concept for Human Mars Exploration," AIAA Paper 2016-0219, January 2016.

[14]Draper, N. R. and Smith, H., *Applied Regression Analysis*, Wiley, New York, 3rd ed., 1998.

[15]Agrawal, P., Prabhu, D., Milos, F. S., and Stackpoole, M., "Investigation of Performance Envelope for Phenolic Impregnated Carbon Ablator (PICA)," AIAA Paper 2016-1515, January 2016.

[16]Daryabeigi, K., Cunnington, G. R., Miller, S. D., and Knutson, J. R., "Combined Heat Transfer in High-Porosity High-Temperature Fibrous Insulations: Theory and Experimental Validation," AIAA Paper 2010-4660, June 2010.

[17]Seiferth, R. W., "Ablative Heat Shield Design for Space Shuttle," NASA CR-132282, August 1973.

[18]Chen, Y. K. and Milos, F. S., "Ablation and Thermal Response Program for Spacecraft Heatshield Analysis," *Journal of Spacecraft and Rockets*, Vol. 36, No. 3, May-June 1999, pp. 475–483.

[19]Brune, A. J., West, IV, T. K., Hosder, S., and Edquist, K. T., "Uncertainty Analysis of Mars Entry Flows over a Hypersonic Inflatable Aerodyanmic Decelerator," *Journal of Spacecraft and Rockets*, Vol. 52, No. 3, May-June 2015, pp. 776–788.

[20]Bose, D. M. et al., "The Hypersonic Inflatable Aerodynamic Decelerator (HIAD) Mission Application Study," AIAA Paper 2013-1389, March 2013.

[21]Anon, *MSC Nastran 2012.2 Quick Reference Guide*, MSC Software Corporation, Santa Ana, CA, 2012.

[22]Anon, *MSC Nastran 2014.1 Design Sensitivity and Optimization User's Guide*, MSC Software Corporation, Santa Ana, CA, 2014.

[23]Bushnell, D., Almroth, B. O., and Sobel, L. H., "Buckling of Shells of Revolution with Various Wall Constructions," NASA CR-1050, May 1968.

[24]Stein, M., "Large Sample Properties of Simulations Using Latin Hypercube Sampling," *Technometrics*, Vol. 29, No. 2, May 1987, pp. 143–151.